

Progress of photonic crystal fibers and their applications

Wei CHEN (✉)^{1,2}, Jinyan LI^{1,2}, Peixiang LU¹

¹ Wuhan National Laboratory for Optoelectronics, Huazhong University of Science and Technology, Wuhan 430074, China

² State Key Laboratory of Optical Communication Technologies and Networks, Optical Fiber Department of Fiberhome Telecommunication Technologies Co., Ltd., Wuhan 430074, China

© Higher Education Press and Springer-Verlag 2009

Abstract In this article, the fabrication technologies of photonic crystal fibers (PCFs) and their applications at home and abroad were formulated at length, especially in fields such as large mode-area active PCFs, fiber lasers, birefringence fibers, sensors, high nonlinear PCFs, frequency transformation, dispersion compensation PCFs, wideband communication for optical network systems, and photonic band-gap fibers. Finally, according to the above analysis, the prospects and developing trends of PCFs were presented.

Keywords photonic crystal fiber (PCF), fabrication, fiber laser, optoelectronic devices

1 Introduction

Photonic crystal fibers (PCFs) [1,2], known as micro-structured optical fibers or holey fibers, have attracted worldwide interest within the last decade due to their unique optical properties with a much higher degree of design freedom compared to conventional optical fibers. These new and fascinating properties have fuelled the desire to make more efficient fiber lasers, light sources, dispersion compensating modules, optical sensors as well as new fiber devices using PCF technology [3–7]. PCFs are characterized by a pattern of micrometer-sized air-holes along the entire length of the fiber. The most common names for addressing these fibers are index-guiding PCF and photonic band-gap (PBG) fiber, which also indicate their guiding mechanisms. The former mechanism is similar to conventional optical fibers with the total internal reflection effect, in which the refractive index of the core is larger than that of the cladding. The latter guides light in the low index core by the band gap effects of the cladding. The different structures endow different characteristics to

the PCFs. For instance, PCFs with a hollow core present a bandgap property, but it has difficulty in getting a low loss; in contrast, all-solid PCFs with a low index core are easily manufactured and have low attenuation in telecommunication windows. Moreover, they can be spliced with conventional optical fibers and are more practical in real application. PCFs with index-guiding have a high index solid core and can easily get a low attenuation. At present, many kinds of PCFs have been manufactured and commercialized for practical use. In this paper, the progress of PCFs in international research is formulated in detail and their developing trends are also presented.

2 Fabrication techniques of PCFs

The fabrication technologies of PCFs vary from different base materials, and the different preparing techniques should be suitable for different materials. The materials for PCFs include polymers such as poly-methylmethacrylate (PMMA), silica glass and multiple components glass. Polymer materials have a lower melting point and are easily processed [8]. However, air-holes in polymers are prone to deform, and the high attenuation of polymers limits their developments. Silica glass materials have a high melting point and thus need professional equipment to treat with. In view of their good optical performances, the materials are all generally adopted. In contrast to silica glass materials, multiple-component glass has lower machining temperature, and thus allows air-holes to maintain a good shape. This kind of material has been applied for some special ions-doped PCF. However, their optical characteristics are not as good as those of silica glass materials. At present, silica glass remains the general and popular material for PCFs.

Polymer PCFs could be directly manufactured by injection molding, sol-gel casting with different structural molders, and extrusion with a metal die in the plastic extruders and drilling because the polymer has a lower

melting point and low hardness. Large et al. have fabricated a kind of graded index microstructured polymer optical fibers which can transmit 1 Gb/s of data over 100 m [9].

However, since the melting temperature of glass is much higher than that of polymer, preparing techniques of polymer PCFs generally are not suitable for glass PCFs. The most popular techniques for this kind of glass PCFs include the stacking-and-drawing method of capillaries and rods, and the method of drilling holes in large diameter fiber preforms. Multiple component bulk glass could be easier to make than the silica at lower temperature, because silica glass has a much higher melting point. However, the PCFs of silica glass also have many advantages, including low attenuation across a wide wavelength range. In addition, since they are currently at the forefront of PCF development, their fabrication techniques should be given emphasis and practically formulated.

The most widely-used fabricating technique is stacking circular capillaries, which has merits such as flexible design, convenient operation, and easier-to-fabricate complex structured PCFs. The operational process is as follows: first, high-purity synthetic silica capillaries or rods with lower hydroxyl content and high clarity in the wide wavelength range with outer diameters of about 1 mm are drawn. The ratio of inner diameter to outer diameter of the capillaries typically lies in the range from 0.20 to beyond 0.95. The uniformity in diameter and circularity of the capillaries should be controlled to at least 1% of the outer diameter. They are stacked horizontally in a suitably shaped jig to form the desired crystalline array. The stack array is then inserted into a jacket tube, thus forming the PCF preform. The whole assembly is then mounted on the horizontal lathe to solidify their structures in case of deformation. The PCF preform is then mounted onto the drawing tower for drawing down to fiber at a processing temperature of about 2100°C. As drawing progresses, judicious pressure and appropriate vacuum in the fiber preform should be adjusted and properly maintained so that the final structural parameters of PCF could be precisely controlled and uniformity along the fiber axis is ensured. In practice, the controlling parameter of the drawing process must have a certain tolerance to allow the formation of certain structures in the PCFs.

3 Applications of PCFs

With the major breakthrough on the attenuation of PCFs, the fibers would be commercialized, making their application broader. At present, the study on the attenuation of PCFs has made great progress. The attenuation at 1310 and 1550 nm for total internal reflection (TIR) PCFs is 0.35 dB/km and 0.205 dB/km, respectively [10], which is nearly the same level as the common single-mode optical fibers. The hydroxyl absorption at 1383 nm is below

1.0 dB/km [11]; the attenuation for hollow core PBG fibers is decreased from 1.7 to 1.2 dB/km at 1620 nm [12]. The main applications of PCFs are formulated in the following.

3.1 Active large mode-field area PCF and fiber laser

Active large mode-field area (LMA) PCFs are the most significant application in the field of fiber lasers. Since it is incompatible to obtain good laser beam quality with LMA for common active fiber lasers, the core diameter must be increased to raise laser power. Meanwhile, the core numerical aperture (NA) of active fibers should be decreased to maintain good laser beam quality. However, this method has its limitations. In addition, decreasing NA of the active fiber core would decrease the rare-earth doping concentration and laser slope efficiency. The endless single-mode (ESM) performance of PCF could tackle this paradox.

The ESM properties of PCFs are different from those of the common standard single-mode optical fibers [13–15], e.g., they have a very wide single-mode operating wavelength range in spite of a larger core diameter. Light could be kept at single-mode performance given the condition of LMA. ESM has properties advantageous to attaining good beam quality for high power fiber laser. The large mode field is good for reducing the nonlinear effect and transmitting higher laser power. Good thermal dissipation performance for high power fiber laser could be achieved by using large mode field PCFs simultaneously. Raising fiber transmission power and obtaining good beam quality are both hotspots in the high power laser fields.

Based on this characteristic of PCFs, LMA PCFs were successfully designed and fabricated. A single LMA ytterbium-doped PCF with a 1.53 kW continuous-wave (CW) laser power has been achieved [16]. The beam quality factor M^2 is less than 3, which is the maximum power output of active PCF with LMA at present. In the experiment, the core diameter of the LMA PCF was 31 μm . In 2003, an LMA rod PCF laser with 60 μm core diameter was made by Jena institute. The fiber's mode area was as large as 2000 μm^2 , with an absorption coefficient as high as 30 dB/m [17] and slope efficiency of 78%. The ytterbium ion concentration varied from 3000 to 12000 ppm with different measuring methods [18]. The concentration of ytterbium ions was therefore proven by the absorption coefficient in practice. Recently, fiber lasers have entered into the realm of kilowatt power with diffraction-limited beam quality.

On the other hand, how much pump light can be coupled into the inner cladding of a double-clad fiber depends on the inner cladding size and its NA. The NA of inner cladding for double-cladding rare-earth doped optical fiber could be raised significantly by using microstructuring techniques, i.e., the inner cladding waveguide can be surrounded by an outer array of air-silica compounded

structures, which would result in a very large effective index contrast. Thus, a higher NA of inner cladding could be achieved, which makes it easy to launch light from a high-power laser diode into the double-cladding rare-earth doped optical fiber. In theory, the numerical aperture could be enlarged to above 1.0. Nevertheless, a double-cladding ytterbium-doped optical fiber with inner-cladding NA of 0.8 has already been manufactured [17,19]. The higher the inner-cladding NA, the larger the acceptance angles, which can raise the coupling efficiency of pump laser diodes and decrease the cost of producing fiber lasers.

Figure 1 shows the cut scanning electron microscope (SEM) images for the two kinds of double-cladding ytterbium-doped PCFs [17,20]. The core of PCF A, doped with 0.6 wt% ytterbium ions, has 0.05 core NA and is 28 μm in diameter. The air-cladding has 42 bridges with a bridge width of 400 nm and bridge length of 50 μm . The inner-cladding NA of 0.55 is achieved. PCF B is another typical double-cladding ytterbium-doped PCF. The seven missing-holes in the center are substituted by an ytterbium-doped rod, and a core diameter of 50 μm and core NA of 0.03 are obtained [21]. The inner-cladding NA is 0.62 at 950 nm. The beam quality factor M^2 of 1.2 was achieved.

The double-cladding ytterbium-doped PCFs were fabricated by Fiberhome Telecommunication Technologies Co., Ltd. The 3.96 W output laser power at 1080 nm was obtained with a 915 nm pump laser diode, the slope efficiency was 79.6% and the light-light transformation efficiency was 76.2% with a 0.8 m long ytterbium-doped PCF.

Overall, due to the unique performance of active PCFs, they would significantly invigorate the high power laser and have the potential to revolutionize the rare-earth doped fiber laser in high power operation.

3.2 Birefringence microstructured optical fiber and devices

Birefringence microstructured optical fibers could be used in many device fields because they have high birefringence and are not sensitive to variations in temperature. All kinds

of asymmetries could be introduced into optical fibers by one or more asymmetric fiber cores and by careful positioning of capillaries with the same external diameter. However, different wall thicknesses lead to different hole sizes in the cladding of the final fiber, with which high modal birefringence could be obtained.

Theoretically, the modal birefringence B of photonic crystal polarization maintaining optical fibers (PC-PMFs) could reach the 1×10^{-2} level for high birefringence index-guiding PCFs [22]. In fact, PC-PMFs with a modal birefringence $B = 1.2 \times 10^{-3}$ have been exploited [23]. The highly birefringent PCF with a hollow core has also been fabricated [24] with a group birefringence of 2.5×10^{-3} at 1550 nm.

The structural birefringence properties of the hollow-core photonic band-gap fiber were carefully investigated and applied to all-fiber chirped-pulse amplification as a compressor. An ultrafast all-optical switch using pulse trapping by an orthogonally polarized soliton pulse in birefringence fiber was also investigated [25]. The fiber exhibits a modal birefringence of 1.2×10^{-3} at the wavelength of 1.24 μm , which allows polarization switching of the central wavelength of its blue-shifted output by 75 nm. The high speed 10 Gb/s optical transmission experiment has been successfully demonstrated in a low-loss PC-PMF, with fiber loss and modal birefringence at 1550 nm are 1.3 dB/km and 1.4×10^{-3} [26], respectively. Corning Company fabricated a single-polarized holey fiber [27]. The hole-assisted single polarization fibers have a cutoff wavelength for each of the two fundamental polarization modes, which could result in significantly different behaviors. The fiber's property could be variable for end users in different deployed conditions. Temperature-insensitive strain measurement was realized by using a polarization-maintaining PCF Sagnac interferometer, and the achieved sensitivity was 0.23 $\text{pm}/\mu\epsilon$ [28]. Delgado-Pinar et al. fabricated an endlessly single-mode anisotropic microstructured fiber with a group birefringence $B_g = 2.1 \times 10^{-3}$ at 1.55 μm [29].

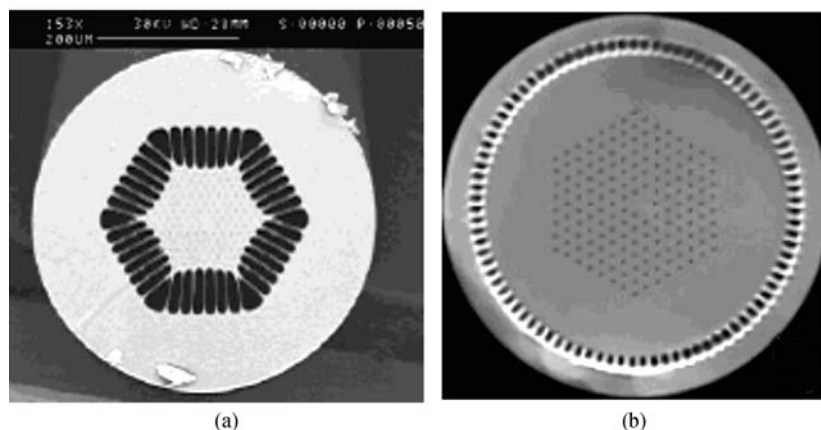


Fig. 1 Cut images for two kinds of double-cladding ytterbium-doped PCFs. (a) PCF A; (b) PCF B

3.3 Highly nonlinear PCF and frequency transformation

The super-continuum spectrum and frequency transformation could be obtained by using highly nonlinear PCFs, even with pumping power two orders lower than the launching power into common nonlinear optical fibers [30]. Besides, it is possible to shift the zero dispersion wavelength of single-mode fiber to much shorter wavelength in PCFs, for example, shifting to the wavelength range from 670 to 880 nm [31]. However, it is impossible to move the zero dispersion wavelength of a silica step-index single-mode optical fiber to shorter than 1290 nm. This special performance of small-core high-index contrast PCFs could be exploited to have dramatic effects on the super-continuum generation of the Ti:sapphire femto-second laser systems with zero dispersion wavelengths in the range of 750–850 nm. It was reported that this single broadband light source exploited with highly nonlinear PCFs could provide 1000 signal light sources for a dense wavelength division multiplexing (DWDM) optical communication system [32].

It is very flexible to design and fabricate small-core and high-index contrast PCFs as the introduction of many air-hole arrays. The filling fraction of air-holes in the optical fiber will decide the effective index of fiber cladding, but will also restrict the distribution of light wave fields in the optical fiber core [33–35]. When the air-filling fraction is very large, near or even above 95%, the light field would be firmly restricted in the small core, and the nonlinear coefficient of optical fibers will increase significantly. When the intensive laser pulse power acts on nonlinear media, several different frequencies interact and generate light with new frequencies [36]. The more intensive the interaction, the broader the spectrum, so the broadband super-continuum spectrum can finally be obtained for a certain wavelength range.

A kind of highly nonlinear PCF was made by Fiberhome as shown in Fig. 2. Its nonlinear coefficient was as high as $112 \text{ (W}\cdot\text{km)}^{-1}$ and the zero dispersion wavelength was 1120 nm. However, the fiber has a negative dispersion of $-88 \text{ ps}/(\text{nm}\cdot\text{km})$ at 800 nm as well as a negative dispersion in the region of 580–900 nm pumping wavelengths. When the pumping pulses are launched close to the zero-dispersion wavelength of the nonlinear PCF, the introduction of the nonlinear PCFs leads to a super-continuum generation. In general, fiber dispersion plays a key role in short pulse propagation and in phase matching conditions for nonlinear processes. The broadly spanning super-continuum emission with a smooth spectrum stretching from 450 to 1400 nm was obtained by the injection of the 30-fs Ti:sapphire laser pulses into the 2 m long high linear PCFs, with energy of up to 5 nJ and a central wavelength of 800 nm at a pulse repetition rate of 100 MHz. Tianjin University conducted an experiment with the nonlinear PCF, where the injection peak power was 0.8 kW, the spectrum intensity was low and the

spectrum was narrow and coarse as shown by the curve A in Fig. 3. After a further increase in the pulse peak power to 5 kW, the spectrum was promptly widened with the wavelength range from 400 to 1400 nm as shown by curve B in Fig. 3. However, the red shift and blue shift spectrum intensity was still low. At the same time, there was an obvious dip at 1000 nm in the curve. While the injection pulse peak power was increased to 10 kW, the smooth features and spectrum intensity were greatly improved as shown by curve C in Fig. 3. If germanium or other materials were doped into fiber core, the nonlinearity of the PCF would be greatly enhanced, and a much broader and smoother super-continuum spectrum could be obtained. Highly nonlinear PCFs will be widely applied in the fields of broadband light sources, optical coherence tomography, high precision frequency measurement, dispersion testing and biomedical treatment.

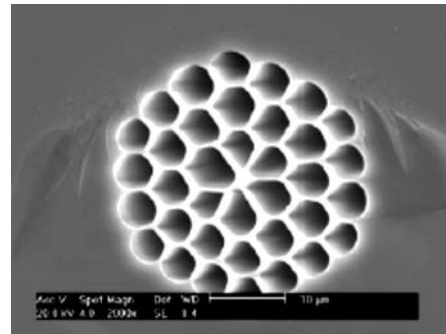


Fig. 2 SEM image of highly nonlinear PCF

3.4 Dispersion compensation PCF and dispersion compensation

It is low-cost and efficient to broaden the transmission capacity by increasing the data rate and channel counts based on the established G. 652 optical networks to meet ever-increasing demand for communication bandwidth. However, in such systems the chromatic dispersion of transmission optical fiber is one of the primary limits. One of the best approaches to minimize the penalty of the chromatic dispersion is to use dispersion compensating fiber (DCF). The basic design of the DCF consists of two spatially separated asymmetric concentric cores with matched cladding [37]. This structure supports two supermodes: the fundamental supermode and second supermode. Commercially available DCF modules are based on the fundamental supermode. To achieve a large negative dispersion and ensure single-mode transmission, the fiber core should have a high refractive index and a small diameter. As a result, the effective fiber mode field area is small. The typical effective area is around $15\text{--}20 \mu\text{m}^2$. Because of the limitation of the doping concentration, large dispersion values cannot be realized in conventional DCFs.

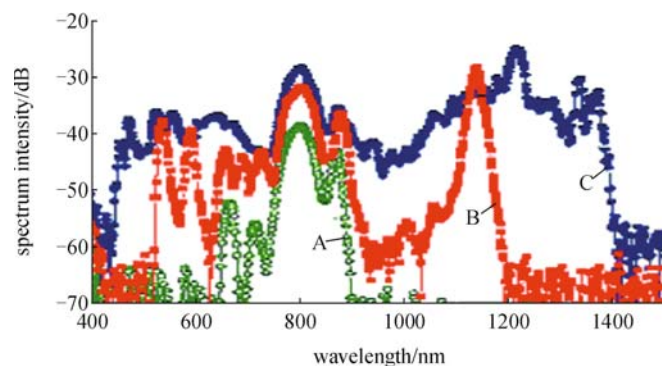


Fig. 3 Super-continuum obtained by highly nonlinear PCF with 30-fs Ti:sapphire laser pulses at peak power (A: 0.8 kW, B: 5 kW, C: 10 kW)

The typical dispersion value is about -100 – -150 ps/(nm·km).

PCFs can realize a larger refractive index modulation than conventional silica optical fibers, which can afford more knobs to tailor PCF dispersion. Many works have been carried out to obtain a large waveguide dispersion in PCFs. Gerome originally used PCF technology to realize the coupling asymmetric dual-core structure commonly used in commercial DCF design. By introducing a ring of air-holes with smaller diameter in the outer ring core, the dual-core asymmetry structure based on pure silica was achieved. This structure can exhibit a high negative chromatic dispersion of -2200 ps/(nm·km) at 1550 nm. Yang et al. in Tsinghua University designed a kind of dual-core structured PCF (DC-PCF), shown in Fig. 4, and it was successfully fabricated by Fiberhome Telecommunication Technologies Co., Ltd. Figure 5 shows that the peak dispersion value of this PCF is -666.2 ps/(nm·km) [38,39]. The position of the dispersion peak is at the wavelength of 1586 nm, which has a shift from the designed peak position.

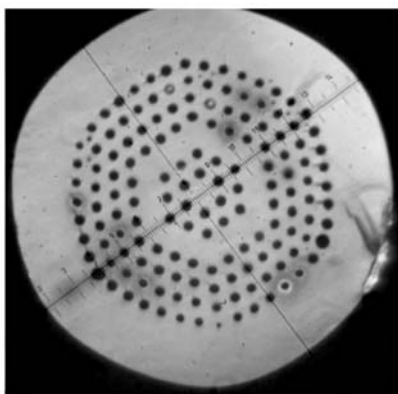


Fig. 4 DC-PCF SEM

In theory, the highly negative dispersion PCF with -55000 ps/(nm·km) at 1550 nm could be designed, but

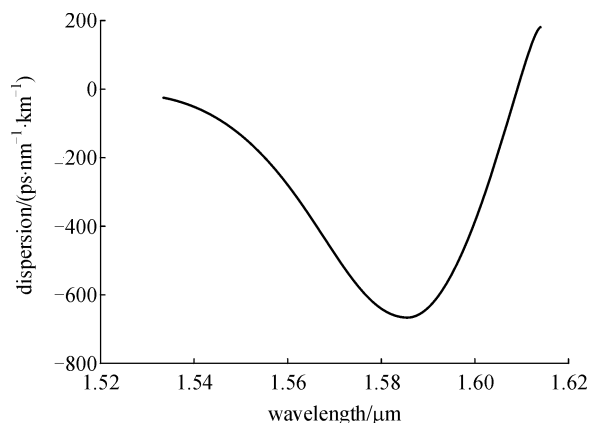


Fig. 5 Dispersion curve of DC-PCF

difficult to operate in practice. Therefore, the theoretical design should be technically feasible. In addition, the uniformity of fiber waveguides is also important because the non-uniform diameter of the holes, the abnormality of the hole arrangement and a slight longitudinal non-uniformity can lead to a broadening of bandwidth and decrease the absolute value of the peak dispersion.

3.5 PBG fibers (hollow-core and solid core PCF)

The light guiding mechanism of PBG optical fiber is different from that of the total internal reflection PCF. It is analogous to the electronic energy band-gap in semiconductors. While the photons fall into the wells of the photonic band-gap, the photons will be trapped and will only go forward in the band-gap. The first hollow-core PCF was reported in 1999, the core of which was formed by omitting seven capillaries from the pre-form stack, and a hollow core was made by removing 19 missing capillaries from the stack array. The PCF cut image shown in Fig. 6 was fabricated by Crystal-Fiber Company.

In hollow-core PCFs, guidance only occurs when a PBG coincides with a core resonance, which means only restricted bands of wavelength are guided. To obtain PBG in a air-silica PCF, it is necessary to obtain larger air-

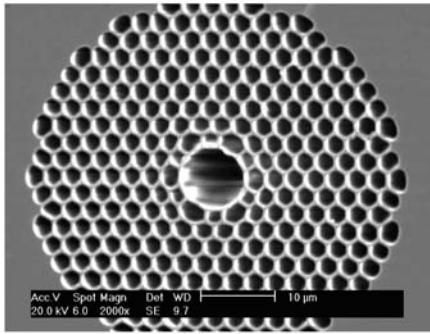


Fig. 6 Hollow-core PBG air-silica fiber

filling fractions and small diameter inter-holes. Therefore, the transmission constant β could be smaller than wavelength vector k in the band region. The key difficulty to resolve for hollow-core PBG fibers is to reduce the leak mode loss, because for particular wavelengths, the phase velocity of the light in the core is not coincident with any phase velocity available in the transmission bands created by the nearest neighbor coupling between rod modes. Thus, light is unable to couple and remains trapped in the core. Similar guided modes are commonly seen in hollow-core PCFs, where surface states can form on the rim of the core and be confined on the cladding side by PBG effects. These surface states then become phase-matched to the air-guided mode at certain wavelengths, creating couplings which can perturb group velocity dispersion and contribute to additional attenuation. Since leak mode loss is the most influential factor for the hollow-core PBG fibers, measurements should be adopted to decrease the leak mode loss of PCFs. Reducing the rim around the hollow core and raising the air-filling fraction are the feasible solutions. At present, the attenuation at 1550 nm wavelength has been reduced to below 10 dB/km [12]. Murao et al. designed a kind of single-mode air-guiding PBG to satisfy the anti-resonant condition, which can operate in a single-mode fashion over a wide wavelength range [40]. Skorobogatiy et al. fabricated ferroelectric all-polymer hollow Bragg fibers for THz guidance, which presented the lowest possible transmission loss from 0.8 to 3.0 THz [41].

In all-solid band-gap PCFs, the core surrounded by an array of high-index germanium doped silica glass strands is made from pure silica. Because the average core-cladding index contrast is negative, total internal reflection could not be realized, making PBG effects the only possible guidance mechanism. Bigot et al. presented a 2D solid-core-PBG ytterbium-doped fiber with the third-order bandgap centered on the 915 nm pumping wavelength [42]. Taru et al. proposed Raman gain suppression by the PBG structure in all-solid PBG fiber used in high power laser delivery without power depletion by Raman process in the fiber [43]. A Bragg fiber with the zero dispersion wavelength shifted towards 1 mm has been fabricated, and

the dispersion of 60 ps/(nm·km) has been achieved at 1064 nm with an optical loss of 1.1 dB/m [44]. Goto et al. demonstrated a wide-band low-loss (< 4 dB/km at 1520 nm) solid PBG fiber [45]. Figure 7 shows a kind of bending insensitive all-solid PBG fiber made by Fiberhome Telecommunication Technologies Co., Ltd., which has an obvious band-gap with an attenuation of 5 dB/km at 1550 nm.

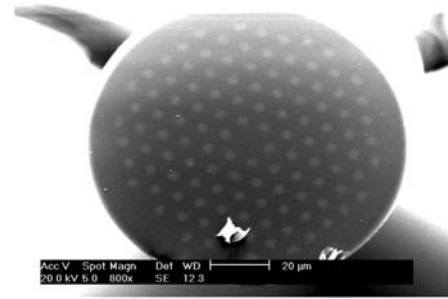


Fig. 7 All-solid PBG silica fiber

3.6 PCF for optical communication systems

With the progress on fabrication techniques, the loss of PCFs has been greatly reduced to 0.205 dB/km [10], and the strength of PCFs was no longer a problem for practical use [46]. Besides the applications in the optical devices, PCFs are also very attractive transmission media for optical communication systems. Stach et al. fabricated a kind of multimode PCF and achieved an experiment of 10 Gbit/s digital data signal transmission [47].

Although PCFs have endless single-mode characteristics and are capable of excellent dispersion tailoring, these unique features cannot be achieved by conventional single-mode optical fibers. The ultra wide single-mode region of PCF has provided the possibility of a 1000 nm band in PCF for 40 Gb/s optical communication [48–50]. With flat chromatic dispersion, a large effective mode area and low leakage losses, a new kind of PCF has been proposed for the S + C + L telecommunication band. However, the fabrication of the proposed PCF topology is still a technological challenge [51,52].

Moreover, the introduction of air-holes in the holey optical fibers could significantly reduce the bending loss of optical fiber effectively, which is very beneficial to the application fields of fiber to the home (FTTH). Because such bending may induce a severe additional loss, it is necessary to solve the problem in the real FTTH field. For conventional single-mode optical fibers, the bending loss increases significantly under a bending radius of 7.5 mm or less, which may result in failure of the optical signal transmission. However, the bending optical loss of the holey optical fibers can be less than 1% that of the conventional single-mode optical fiber, and a kind of high

quality holey fiber has been achieved with low bending loss of less than 0.04 dB/turn under a bending radius of 2.5 mm at the wavelength of 1.55 μm [53]. Kurashima et al. described the development of premises optical wiring components using hole-assisted fiber [54]. The anti-bending characteristic of holey fibers is attractive for flexible optical wiring with the potential for easy and economical in-house installations.

4 Prospects

Due to the remarkable and unique properties of PCFs, their applications will expand in the future, especially in the following fields.

First, the flexible and tailoring dispersion characteristics can be used to fabricate low dispersion flat optical fibers with major advantages for a 40 Giga bit per second (GPS) light transmission system, which could be applied to light communication of high speed, large capacity long distance systems. Second, the holey fibers with air-holes show significant anti-bending performance. In the small bending radius they have significantly lower bending loss compared with the common single-mode optical fiber. The FTTH will need a high number of this kind of bending-insensitive PCF, for example, in Japan the bending-insensitive PCFs have been used in fiber to the desk fields. Third, by using the highly nonlinear effect of PCFs, the 100 nm super-continuum spectrum has been obtained, and they could also be used for wavelength transformation devices. Radio over fiber technology with high nonlinear PCFs could be used in the field of cryptology of telecommunication. Fourth, LMA ytterbium-doped PCFs will be extensively applied to high power fiber lasers, which have been widely used in laser marking and laser cutting fields. Fifth, different optical devices and sensors with PCFs have a great potential and will create an attractive market. Last, but not least, great progress has been made on slow light research with high nonlinear PCFs, which will provide another feasible technology for light storage and all-optical communication. Overall, PCFs have a bright and promising future.

Acknowledgements This work was supported by the National Basic Research Program of China (Grant No. 2003CB314905), the National High Technology Research and Development Program of China (Grant No. 2007AA03Z447) and the National Key Basic Research Special Foundation (Grant No. 2006CB806006).

References

1. Kaiser P, Astle H W. Low-loss single-material fibers made from pure fused silica. *The Bell System Technical Journal*, 1974, 53(6): 1021–1039
2. Birks T A, Roberts P J, Russell P S J, et al. Full 2-D photonic bandgaps in silica/air structures. *Electronics Letters*, 1995, 31(22): 1941–1943
3. Cregan R F, Mangan B J, Knight J C, et al. Single-mode photonic band gap guidance of light in air. *Science*, 1999, 285(5433): 1537–1539
4. Knight J C, Birks T A, Russell P S J, et al. All-silica single-mode optical fiber with photonic crystal cladding. *Optics Letters*, 1996, 21(19):1547–1549
5. Birks T A, Knight J C, Russell P S J. Endlessly single-mode photonic crystal fiber. *Optics Letters*, 1997, 22(13): 961–963
6. Russell P S J. Photonic crystal fibers. *Science*, 2003, 299(5605): 358–362
7. Kumar V V R K, George A K, Knight J C, et al. Tellurite photonic crystal fiber. *Optics Express*, 2003, 11(20): 2641–2645
8. Ebendorff-Heidepriem H, Monro T, van Eijkelenborg M A, et al. Extruded polymer preforms for high-NA polymer microstructured fiber. In: *Proceeding of OFC/NFOEC'2006, Anaheim*. 2006, OThH4
9. Large M C J, Lwin R, Manos S, et al. Experimental studies of bandwidth behaviour in graded index microstructured polymer optical fibres. In: *Proceeding of ECOC2007, Berlin*. 2007, Session 4.1.3
10. Yao B, Ohsono K, Kurosawa Y, et al. Low-loss holey fiber. In: *Proceedings of the 53rd IWCS/Focus, Pennsylvania*. 2004, 135–139
11. Tajima K, Kurokawa K, Nakajima K, et al. Toward transmission applications with microstructured fibers. In: *Proceedings of OFC/NFOEC'2006, Anaheim*. 2006, OThH1
12. Roberts P, Couny F, Sabert H, et al. Ultimate low loss of hollow-core photonic crystal fibres. *Optics Express*, 2005, 13(1): 236–244
13. Saitoh K, Tsuchida Y, Koshiha M, et al. Endlessly single-mode holey fibers: the influence of core design. *Optics Express*, 2005, 13(26): 10833–10839
14. Birks T A, Knight J C, Russell P S J. Endlessly single-mode photonic crystal fiber. *Optics Letters*, 1997, 22(13): 961–963
15. Mortensen N A, Folkenberg J R, Nielsen M D, et al. Modal cutoff and the V parameter in photonic crystal fibers. *Optics Letters*, 2003, 28(20): 1879–1881
16. Bonati G, Voelckel H, Gabler T, et al. 1.53 kW from a single Yb-doped photonic crystal fiber laser. In: *Proceeding of Photonics West: Late Breaking Developments*. San Jose, 2005, Session 5709-2a
17. Limpert J, Schreiber T, Nolte S, et al. High-power air-clad large-mode-area photonic crystal fiber laser. *Optics Express*, 2003, 11(7): 818–823
18. Lavoute L, Roy P, Desfarges-Berthelemot A, et al. Design of microstructured single-mode fiber combining large mode area and high rare earth ion concentration. In: *Proceeding of OFC2006, Anaheim*. 2006, OFK1
19. François V, Aboutorabi S S. Fracture strength of air-clad microstructured fibers. In: *Proceeding of OFC/NFOEC'2007, Anaheim*. 2007, OThA4
20. Schreiber T, Limpert J, Liem A, et al. Thermo-optical analysis of air-clad photonic crystal fiber lasers. In: *Proceeding of OFC'2004, Anaheim*. 2004, TuA2
21. Limpert J, Liem A, Reich M, et al. Low-nonlinearity single-transverse-mode ytterbium-doped photonic crystal fiber amplifier. *Optics Express*, 2004, 12(7):1313–1319
22. Suzuki K, Kubota H, Kawanishi S, et al. Optical properties of a low-loss polarization maintaining photonic crystal fiber. *Optics Express*,

- 2001, 9(13): 676–680
23. Mitrofanov A V, Linik Y M, Buczynski R, et al. Highly birefringent silicate glass photonic crystal fiber with polarization controlled frequency shifted output: a promising fiber light source for nonlinear raman microspectroscopy. *Optics Express*, 2006, 14(22): 10645–10651
 24. Roberts P J, Williams D P, Sabert H, et al. Design of low loss and highly birefringent hollow core photonic crystal fiber. *Optics Express*, 2006, 14(16): 7329–7341
 25. Islam M N, Poole C D, Gordon J P. Soliton trapping in birefringent optical fibers. *Optics Letters*, 1989, 14(18): 1011–1013
 26. Zhu Z M, Brown T. Experimental studies of polarization properties of supercontinua generated in a birefringent photonic crystal fiber. *Optics Express*, 2004, 12(5): 791–796
 27. Chen X, Li M J, Koh J, et al. Bending properties of hole-assisted single polarization fibers. In: *Proceedings of OFC/NFOEC'2007, Anaheim. 2007, OThA2*
 28. Dong X Y, Tam H Y, Shum P. Temperature-insensitive strain measurement with PM-PCF based Sagnac interferometer. In: *Proceedings of ECOC'2007, Berlin. 2007, Session 3.6.6*
 29. Delgado-Pinar M, Díez A, Torres-Peiró S, et al. Guidance and polarization properties of an anisotropic microstructured fibre. In: *Proceedings of ECOC'2007, Berlin. 2007, Session 7.1.4*
 30. Foster M, Gaeta A. Ultra-low threshold supercontinuum generation in sub-wavelength waveguides. *Optics Express*, 2004, 12(14): 3137–3143
 31. Zhang R, Teipe J, Giessen H. Theoretical design of a liquid-core photonic crystal fiber for supercontinuum generation. *Optics Express*, 2006, 14(15): 6800–6812
 32. Takara H, Ohara T, Mori K, et al. More than 1000 channel optical frequency chain generation from single supercontinuum source with 12.5 GHz channel spacing. *Electronics Letter*, 2000, 36(25): 2089–2090
 33. Varshney S, Fujisawa T, Saitoh K, et al. Novel design of inherently gain-flattened discrete highly nonlinear photonic crystal fiber Raman amplifier and dispersion compensation using a single pump in C-band. *Optics Express*, 2005, 13(23): 9516–9526
 34. Ranka J K, Windeler R S, Stentz A J. Visible continuum generation in air-silica microstructure optical fibers with anomalous dispersion at 800 nm. *Optics Letter*, 2000, 25(1): 25–27
 35. Saitoh K, Florous N, Koshiha M. Ultra-flattened chromatic dispersion controllability using a defected core photonic crystal fiber with low confinement losses. *Optics Express*, 2005, 13(21): 8365–8371
 36. Gorbach A V, Skryabin D V, Stone J M, et al. Four-wave mixing of solitons with radiation and quasi-nondispersive wave packets at the short-wavelength edge of a supercontinuum. *Optics Express*, 2006, 14(21): 9854–9863
 37. Nakajima K, Matsui T, Kurokawa K, et al. High-speed and wideband transmission using dispersion-compensating/managing photonic crystal fiber and dispersion-shifted fiber. *Journal of Lightwave Technology*, 2007, 25(9): 2719–2726
 38. Yang S G, Zhang Y J, He L N, et al. Experimental demonstration of very high negative chromatic dispersion dual-core photonic crystal fiber. In: *Proceedings of OFC/NFOEC'2007, Anaheim. 2007, OThA6*
 39. Yang S G, Zhang Y J, Peng X Z, et al. Theoretical study and experimental fabrication of high negative dispersion photonic crystal fiber with large area mode field. *Optics Express*, 2006, 14(7): 3015–3023
 40. Murao T, Saitoh K, Florous N J, et al. Single-mode air-guiding photonic bandgap fiber with improved broadband transmission characteristics: the benefits of an anti-resonant core design. In: *Proceedings of OFC/NFOEC'2007, Anaheim. 2007, JWA4*
 41. Skorobogatiy M, Dupuis A, Guo N. Design and fabrication of ferroelectric all-polymer hollow Bragg fibers for THz guidance. In: *Proceedings of OFC/NFOEC'2007, Anaheim. 2007, JWA98*
 42. Bigot L, Pureur V, Jaouen Y, et al. Ytterbium-doped 2D solid core photonic bandgap fiber for laser operation at 980 nm. In: *Proceedings of ECOC'2007, Berlin. 2007, Session 1.4.5*
 43. Taru T, Hou J, Knight J C. Raman gain suppression in all-solid photonic bandgap fiber. In: *Proceedings of ECOC'2007, Berlin. 2007, Session 7.1.1*
 44. Likhachev M E, Levchenko A E, Bubnov M M, et al. Low-loss dispersion-shifted solid-core photonic bandgap bragg fiber. In: *Proceedings of ECOC'2007, Berlin. 2007, Session 7.1.2*
 45. Goto R, Takenaga K, Matsuo S, et al. Solid photonic band-gap fiber with 400 nm bandwidth and loss below 4 dB/km at 1520 nm. In: *Proceedings of OFC/NFOEC'2007, Anaheim. 2007, OLM7*
 46. Kosolapov A F, Semjonov S L, Denisov A N, et al. Mechanical strength and fatigue of microstructured optical fibers. In: *Proceedings of OFC/NFOEC'2007, Anaheim. 2007, OThA3*
 47. Stach M, Broeng J, Petersson A, et al. 10 Gbit/s 850 nm VCSEL based data transmission over 100 m-long multimode photonic crystal fibers. In: *Proceedings of ECOC'2003, Rimini, 2003, Th3.3.3*
 48. Kurokawa K, Tajima K, Nakajima K. 10 GHz 0.5 ps pulse generation in 1000 nm band in PCF for high speed optical communication. In: *Proceedings of OFC/NFOEC'2006, Anaheim. 2006, PDP5*
 49. Tajima K, Kurokawa K, Nakajima K, et al. Toward transmission applications with microstructured fibers. In: *Proceedings of OFC/NFOEC'2006, Anaheim. 2006, OThH1*
 50. Kurokawa K, Nakajima K, Tsujikawa K, et al. Penalty-free 40 Gb/s transmission in 1000 nm band over low loss PCF. In: *Proceedings of OFC/NFOEC'2006, Anaheim. 2006, OThH2*
 51. Florous N, Saitoh K, Koshiha M. The role of artificial defects for engineering large effective mode area, flat chromatic dispersion, and low leakage losses in photonic crystal fibers: towards high speed reconfigurable transmission platforms. *Optics Express*, 2006, 14(2): 901–913
 52. Kwok C H, Chow C W, Tsang H K, et al. S/C/L-band wavelength conversion by cross-polarization modulation in a dispersion-flattened nonlinear photonic-crystal fiber. In: *Proceedings of OFC/NFOEC'2006, Anaheim. 2006, OThA4*
 53. Kim G H, Han Y G, Cho H S, et al. A novel fabrication method of versatile holey fibers with low bending loss and their optical characteristics. In: *Proceedings of OFC/NFOEC'2006, Anaheim. 2006, OWI2*
 54. Kurashima T, Hiramoto K, Aoyama H, et al. Potential of hole-assisted fibres in optical access and in-house networks. In: *Proceedings of ECOC'2007, Berlin. 2007, Session 6.1.1*